

Structure and Dynamics of amorphous Silica Surfaces

Alexandra Roder, Walter Kob*, and Kurt Binder

*Institute of Physics, Johannes Gutenberg-University, Staudinger Weg 7, D-55099 Mainz,
Germany*

(November 19, 2000)

Abstract

We use molecular dynamics computer simulations to study the equilibrium properties of the surface of amorphous silica. Two types of geometries are investigated: i) clusters with different diameters (13.5Å, 19Å, and 26.5Å) and ii) a thin film with thickness 29Å. We find that the shape of the clusters is independent of temperature and that it becomes more spherical with increasing size. The surface energy is in qualitative agreement with the experimental value for the surface tension. The density distribution function shows a small peak just below the surface, the origin of which is traced back to a local chemical ordering at the surface. Close to the surface the partial radial distribution functions as well as the distributions of the bond-bond angles show features which are not observed in the interior of the systems. By calculating the distribution of the length of the Si-O rings we can show that these additional features are related to the presence of two-membered rings at the surface. The surface density of these structures is around 0.6/nm² in good agreement with experimental estimates. From the behavior of the mean-squared displacement at low temperatures we conclude that at the surface the cage of the particles is larger than the one in the bulk. Close to the surface the diffusion constant is somewhat larger than the one in the bulk and with decreasing temperature the relative difference grows. The total vibrational density of states at the surface is similar to the one in the bulk. However, if only the one for the silicon atoms is considered, significant differences are found.

PACS numbers: 61.20.Lc, 61.20.Ja, 64.70.Pf, 68.47.Jn

Typeset using REVTeX

*Author to whom correspondence should be addressed to. Permanent address: Laboratoire des Verres, Université Montpellier II, 34095 Montpellier, France, e-mail: kob@ldv.univ-montp2.fr

I. INTRODUCTION

In recent years the structure and dynamics of glass-forming systems has been the focus of many experimental and theoretical investigations [1,2]. These efforts resulted in a current understanding of such systems which is significantly larger than it was just one decade ago, although many properties of glassy systems still remain puzzling. Although so far most studies focused on the bulk properties of these materials, it has become clear that also the surfaces of glassy systems are a very interesting object of research [3,4]. Most studies in this direction have so far concentrated on thin polymer films or the system studied here: silica. Whereas the former type of system is, e.g., frequently applied in coatings, it has been found that amorphous silica surfaces are very reactive and thus can be used in catalysis and chromatography [5–7]. In addition, the properties of such surfaces are also very important in modern materials such as reinforced polymer matrix composites, in metal oxide semiconductor devices, or ultra-light weight nanoporous materials [8,9]. The wide range of these applications has led to numerous studies of the surface using a wide range of methods such as infrared and Raman spectroscopy, atomic force microscopy, as well as NMR [10–19]. These investigations have led to the hypothesis that these surfaces have structural elements that are not present in the amorphous bulk, namely two-membered rings, i.e. two oxygen atoms that are bonded to the same two silicon atoms. Evidence has been given, that it is these short membered rings that form the reaction sites of the surface (in particular with water), thus making them particularly interesting.

Due to the nature of the experiments done to investigate the surfaces, it has so far not been possible to determine the details on the structure of these rings. Therefore efforts were made to use various types of *ab initio* calculations in order to determine their geometry [11,12,20–25]. However, these calculations were usually done for very small clusters or crystalline materials. Since the influence of the surrounding on the geometry of the rings is not understood well, the validity of the so obtained results is unfortunately not very clear. Furthermore these types of calculations have the problem that only very short time scales are accessible (a few ps) and thus the systems cannot be equilibrated at low temperatures. A different approach to investigate the properties of such surfaces is to use classical simulations (Monte Carlo or molecular dynamics (MD)) since they allow to access times scales that are on the order $10^3 - 10^4$ times longer than the one from the quantum mechanical calculations. In order to obtain reliable results from such a simulation it is, however, important to have a potential at hand which is able to describe the effective interactions between the ions reliably. That such types of simulations are indeed possible has been demonstrated in the seminal papers by Garofalini and coworkers [26–32]. In these simulations a potential has been used which was able to describe well several properties of amorphous silica in the bulk. One of the main results of these simulations was that at the surface the frequency of short rings is indeed much larger than the one in the bulk, in agreement with the (indirect) evidence from the experiments. However, due to the way the surfaces in these simulations were created (removing of the boundary conditions in one direction *at low temperatures* in a three-dimensional simulation box), they were not really relaxed, but only annealed. Therefore it was argued that the structure of these surfaces would not correspond to the real ones where a liquid surface is cooled and hence can relax [33]. Further potential difficulties for such types of simulations are discussed in Ref. [34]. Despite these possible problems recently

various types of simulations have been reported in which the structure of the silica surface was investigated as well as its reactivity with water or other small molecules [33,35–37]. What is still lacking, however, is a simulation in which this surface is studied *in equilibrium*, since to our knowledge all previous simulations considered only annealed surfaces. Therefore we will investigate in the present paper the structure of such surfaces and also characterize the dynamics of the atoms. The potential we use is the one proposed some time ago by van Beest *et al.* [38] which has been shown to be very reliable to describe the properties of amorphous silica in the bulk. Below we will argue that this type of potential should also be able to give reasonable results in the vicinity of a surface. Since the structural and dynamical properties of this system in the bulk has in the past been very well characterized, we can make a careful comparison of these properties with the ones of the surface. This comparison will in turn allow us to understand better how the surface influences these properties.

The remaining of the paper is organized as follows: In the next section we describe the model of van Beest *et al.* and give the details on the simulations. In section III we present the results and in the last section we summarize and discuss them.

II. MODEL AND DETAILS OF THE SIMULATIONS

In this section we discuss the model and give the details of the simulations. More details on the latter can be found in Ref. [39].

To gain insight into the structure and the dynamics of a real surface and the transition region between the surface and the bulk by means of computer simulations, it is necessary to have a potential which is able to describe reliably this type of geometry. For the case of silica van Beest, Kramer, and van Santen (BKS) [38] proposed some time ago a potential which turned out to be remarkably good in the description of *bulk properties* of crystalline as well as amorphous SiO_2 [40–44]. Although it is presently not clear to what extent this potential is also reliable in the vicinity of a silica surface, the approach used by BKS to obtain their potential makes one hope that it is also quite reasonable in such a situation, as can be understood as follows: BKS made self-consistent Hartee-Fock calculations to determine the energy surface of *one* H_4SiO_4 tetrahedron, used a certain functional form (described below) to parametrise this surface, and then lattice dynamics calculations to improve further their fit parameters. Thus the initial step in the derivation of the BKS-potential involved also the use of a free surface, although one saturated with hydrogen, and thus it is not unreasonable to expect that the *salient* features of a real silica surface are reproduced by this potential as well. Note that this way to obtain an effective potential is very different from the often used one which involves fitting macroscopic data (density, elastic constants, etc.) and microscopic data (atomic distances, bond-bond angles, etc.) from the *bulk* [29,45], since in the latter approach no surface data is considered.

The functional form of the BKS-potential is given by [38]

$$\phi_{\alpha\beta}(r) = \frac{q_\alpha q_\beta e^2}{r} + A_{\alpha\beta} \exp(-B_{\alpha\beta} r) - \frac{C_{\alpha\beta}}{r^6} \quad \alpha, \beta \in [\text{Si}, \text{O}], \quad (1)$$

where r is the distance between the ions α and β . The value of the parameters q_α , $A_{\alpha\beta}$, $B_{\alpha\beta}$, and $C_{\alpha\beta}$ can be found in Ref. [38]. In order to get a better description of the density in the bulk, the short range part of the potential was truncated and shifted at 5.5\AA [40].

With this model two types of simulations were done: A first one in which a free cluster of silica was studied and a second one in which a thin film was considered, i.e. we used periodic boundary conditions in the x - and y -direction and an infinitely large space in the z -direction [46]. Three different cluster sizes were considered: $N = 436, 1536, \text{ and } 4608$. To generate these clusters we proceeded as follows: We first placed *randomly* the N ions of SiO_2 , in stoichiometric composition, in a sphere of radius R_w at the origin of the coordinate system. The value of R_w was chosen to be substantially larger than a sphere with N ions at the density of amorphous silica (approx. 2.2g/cm^3 [47]), i.e. $R_w = 10, 20, \text{ and } 30\text{\AA}$ for the three system sizes. Due to the randomness, this configuration is very unstable and the ions will accelerate quickly and would escape the spherical region in short time. In order to prevent this we added an external potential at R_w of the form $V_w(r) = (R_w - r_i)^{12}$, where r_i is the distance of particle i from the origin. (The details of this external potential are completely irrelevant, since it is used only at the early stage of the equilibration process.) The equations of motion were then integrated with the velocity form of the Verlet algorithm, using a time step of 1.6fs. To equilibrate the system we coupled the ions to a stochastic heat bath with a temperature T of 4700K. This was done for 5000 time steps which corresponds to several typical relaxation times of the system at this temperature. After this time, the system was equilibrated so far that it had assumed the shape of a drop and the ions did not interact anymore with the external potential. Hence the latter one was switched off and we propagated the particles for additional 10,000 steps in the potential given by Eq. (1). Note that during this equilibration period care was taken that the total momentum as well as the angular momentum were always zero, in order not to put any centrifugal force on the outer particles of the cluster and hence to change the equilibrium structure. The temperatures investigated were 4700K, 4300K, 4000K, and 3400K. In order to improve the statistics of the results we averaged the smallest, medium, and large system over 10, 5 and 3 completely independent runs. In addition we simulated the smallest systems also at 2750K (4 independent samples).

Note that with this geometry we do not have periodic boundary conditions. Hence it is not possible to calculate the long range part of the Coulomb forces by means of the Ewald sum, a technique in which the computational load increases roughly like $N^{1.5}$. Instead it was necessary to make a double loop over all pairs of ions, i.e. the computational load increases like N^2 . Due to this heavy load these kind of investigations are hence only possible by using parallel computers. The total amount of computer time spent for this studies are around 19 years of single processor time on a Cray T3E.

For the simulation of the film we used periodic boundary conditions in the x and y direction. Since the system is not periodic in the z -direction, the usual Ewald summation technique to calculate the long range Coulomb forces cannot be used in this case. Some time ago Parry and Heyes proposed a method how such long range forces can be handled also in a quasi-two dimensional geometry [48,49] and we followed their approach [39]. In analogy to the three dimensional case the forces are decomposed into a sum in real space and one in reciprocal space. Hence also here a parameter α and a maximum cutoff wave-vector k_{max} occur, which we chose to be 0.265 and 6, respectively. The number of atoms were 1152 and in the x and y direction the box had a size of 28.5\AA . As a starting configuration we used a slab of β -cristobalite and melted it at 5200K for 30,000 time steps (49ps). This time was sufficiently long to allow the ions to move on the order of 10\AA , which is large enough

to melt the system completely. The result was an amorphous film with a thickness around 29Å. This system was subsequently cooled and equilibrated at 4300K and 3200K before the production runs were started.

III. RESULTS

In this section we present the results from the simulation of the droplets. After having characterized their general shape, we focus on comparing the structure of the network at the surface with the one in the interior. Finally we will also discuss to what extent the dynamics is affected by the presence of the surface.

Since the size of the droplets are finite it can be expected that their shape is not quite spherical, since fluctuations will give rise to deviations from a sphere on the microscopic level as well as on the length scale of the whole droplet. The size of these fluctuations will in general depend on temperature as well as the size of the system. In order to give an idea on the shape of the droplets we show in Fig. 1 two typical snapshots of the smallest system at two different temperatures. We see that the configuration for the higher temperature, Fig. 1a, has a surface which is very irregular in that many arms point into the vacuum. These arms are formed of silicon atoms that are surrounded by a few oxygen atoms. During the simulations we found that at these high temperatures occasionally the end of such an arm breaks off and becomes detached from the rest of the cluster. These fragments are usually SiO₂ “molecules” and in most cases they fall back onto the cluster at a different place they started from. However, it is clear that occasionally such a fragment will have a velocity high enough to leave the cluster for good and thus will not fall back onto the cluster. Hence, on long time scales the cluster is only metastable, since it will ultimately evaporate. (The same will be true also in the thin film geometry.) However, on the time scale of the simulation we have not observed these processes for $T \leq 4700\text{K}$, but for higher temperatures occasionally a fragment is indeed spawned off to infinity [50].

If the temperature is lowered, most of the mentioned arms disappear and the surface becomes much smoother, Fig. 1b. At these low temperatures only occasionally dangling O-bonds are sticking out from the cluster. However, despite this local smoothness the overall shape of the cluster is far from being spherical, since its surface is still rough at larger length scales. (We emphasize that this roughness is *not* static, since the cluster reconstructs itself on the time scale of a few ns.) Using viscoelastic theory, Jäckle and Kawasaki addressed the problem of the roughness of a supercooled liquid [51]. They predict that this roughness should be given by $k_B\sqrt{T/4\pi\sigma}$, where σ is the surface tension. If we use $T = 3000\text{K}$ and a surface tension of 0.33N/m [47], we obtain a predicted roughness around 1Å, a value which in view of Fig. 1b is very reasonable, and is also in good agreement with experimental data [18].

In order to characterize the shape of the cluster, we have calculated its three principal moments of inertia, and label them according to their magnitude $I_1 \geq I_2 \geq I_3$. In Fig. 2 we show the temperature dependence of the ratios I_1/I_3 and I_2/I_3 , for the three system sizes. From this figure we recognize that the typical shape of the cluster is rather an ellipsoid than a sphere since the ratio of the long axis to the short one is around $\sqrt{1.32} \approx 1.15$ for the smallest cluster and $\sqrt{1.15} \approx 1.07$ for the largest one. This decrease of the ratio with increasing N can be understood as follows: If we assume that Δ , the amplitude of

the capillary waves on the surface, is only a weak function of N , such as e.g. a logarithmic dependence, we expect that the length of the axis is given by $\Delta + a_1 N^{1/3}$, where a_1 is a slowly varying function (with respect to $N^{1/3}$) of N . Hence the ratio I_1/I_3 will scale like $(\Delta + a_1 N^{1/3})^2/(\Delta + a_2 N^{1/3})^2$, where a_2 is also a constant. If one expands this quotient in powers of $N^{-1/3}$ one thus expects that $I_1/I_3 \approx 1 + \text{const.} N^{-1/3}$, and this is indeed what we find within the accuracy of our data. Note that this reasoning holds also for the ratio I_1/I_2 , and indeed we find the same scaling in our data. Finally we mention that since these ratios are independent of temperature within the accuracy of our data, we can conclude that the amplitude Δ is essentially independent of T also. This implies that the surface tension is only a weak function of T , at least in the temperature range considered, and below we will give some indirect evidence that this indeed the case.

Since in this paper we are interested to characterize the properties of the surface, we need a criterion to decide which atoms belong to the surface and which ones belong to the interior. Since the shape of the droplets is not spherical, we approximated it by an ellipsoid which was defined as follows. For any given droplet we constructed an ellipsoid whose ratio of the principle moments of inertia were the same as the one found for this droplet (assuming that the ellipsoid had a uniform mass distribution). The length of the largest axis was chosen such that the droplet just touched the exterior of the droplet. All atoms that were within 5\AA of this hull were defined to belong to the surface. All atoms that had a distance between 5\AA and 8\AA from the hull were defined to belong to a transition zone, and all atoms with a distance larger than 8\AA were defined to belong to the interior of the droplet. In the following we will call the atoms belonging to the interior, to the transition zone, and to the surface also to belong to shell 1, shell 2, and shell 3. Although this choice of the thickness of the surface and the transition zone are somewhat arbitrary, the values are very reasonably, as we will see below.

Finally we mention that we found that the average length of the largest axis is 13.5\AA , 19\AA and 26.5\AA for the smallest, medium, and largest droplet. This length depends only very weakly on temperature, since the thermal expansion coefficient of silica is quite small. Note that this size shows to a high accuracy a $N^{1/3}$ dependence, in agreement to the assumption used before that the overall shape of the droplet does not depend strongly on N .

The next quantity we consider is e_{pot} , the total potential energy per particle. In Fig. 3 we show the temperature dependence of e_{pot} for the three different system sizes. Also included is the data for the bulk, which stems from a simulation of 8016 particles in a cubic box with periodic boundary conditions [42]. We see that the energy for the clusters is significantly higher than the one of the bulk which is reasonable since the former include also the surface energy S . We thus expect the relation

$$\Delta e_{\text{pot}} \equiv e_{\text{pot}}(N) - e_{\text{pot}}^{\text{bulk}} = \frac{\epsilon S}{N} \quad (2)$$

$$\propto \epsilon N^{-1/3} \quad , \quad (3)$$

where ϵ is the surface energy per unit area, and in the second equality we have assumed that the shape of the cluster is independent of T , which in view of the results presented in Fig. 2 is very reasonable. Note that ϵ is *not* the surface tension σ , since the latter gives the excess per unit area of the *free* energy. Thus we have $\epsilon \geq \sigma$, due to the entropic contribution to the free energy.

According to Eq. (3) the N -dependence of Δe_{pot} should be $N^{-1/3}$. That this is indeed the case is demonstrated in the inset of Fig. 3 where we plot this quantity for two temperatures. The value of ϵ can thus be estimated from Δe_{pot} via Eq. (2) by assuming that the droplet is a sphere of radius R_0 and hence its surface is $4\pi R_0^2$. For $T = 3000\text{K}$ we find for all three system sizes $\epsilon = (0.7 \pm 0.1)\text{N/m}$, where we have taken for R_0 the value of the largest axis of the above mentioned ellipsoid.

From Eq. (2) it is clear that the T -dependence of Δe_{pot} can have two origins: The T -dependence of ϵ and the one of S . Above we have argued, using the results of Fig. 2, that this latter T -dependence is only weak, a conclusion that we will confirm below. Therefore we can calculate the T -dependence of ϵ from the one of Δe_{pot} , see Fig. 3. The results are shown in Fig. 4. We see that ϵ decreases with increasing temperature, in agreement with experimental findings *for the surface tension* [47]. The slope that we find is $-(17 \pm 9) \cdot 10^{-3}\text{N/m}$ per 100K, which compares well with the estimate from experiments which is around $-10 \cdot 10^{-3}\text{N/m}$ per 100K for σ [47]. We also mention that the experimental value of σ around 2000K is $0.33 \pm 0.04\text{N/m}$ [47], i.e. it is around a factor of three smaller than an extrapolation of ϵ to this temperature. Since we have argued above, that ϵ must be larger than σ , we thus find that our result for ϵ is quite reasonable.

We now investigate the structure of the clusters in more detail. One important structural quantity is the dependence of the particle density $\rho(r)$ on the distance r from the center of the droplets. To calculate $\rho(r)$ we determined for each configuration the principal axes of the enclosing ellipsoid, see description above. We then constructed a sequence of ellipsoids that were centered at the center of gravity of the cluster, had the same geometrical shape, and whose smallest axis increased in steps of 0.15\AA . We then counted the number of atoms in each shell formed by two consecutive ellipsoids and normalize it by its volume. In Fig. 5 we show the so obtained density distribution at $T = 3000\text{K}$ for the intermediate and largest system (bold and thin curves, respectively). We see that at distances that are a few \AA smaller than the radius of the cluster, e.g. $r \leq 18\text{\AA}$ in the case of $N = 4608$, the total density is constant to within the accuracy of the data, and is independent of N . This density is around 2.3g/cm^3 , the same value that was found for this model in the bulk around zero pressure [40,42]. Thus we have a first evidence that in the interior of the cluster the structure is similar to the one in the bulk.

In the region close to the boundary of the cluster the total density has a small peak. If one looks at the partial densities for silicon and oxygen separately, solid and dashed lines, respectively, one sees that this feature is more pronounced for the case of silicon. The reason for this is that for the system it is energetically better to have an oxygen atom at the surface, since in that way only one bond, if any, has to be broken (i.e. the system forms a dangling bond), whereas if a silicon is at the surface several bonds have to be broken. Thus one expects that the density profile for the oxygen atoms extend to larger distances than the one for silicon, and this is indeed what can be read off from the figure. Due to the excess of oxygen at the surface, the tendency to achieve local charge neutrality makes it now very likely that the layer just below the surface has an excess in silicon, thus rationalizing the peak in the total density. A qualitatively similar behavior has been found by Garofalini and coworkers for a different potential [32] which shows that this oxygen enrichment is not an artifact of the present model.

That this effect can also be seen in the thin film is demonstrated in Fig. 6, where we show

the density profile for this type of geometry. The two lower curves are the densities for the oxygen and silicon atoms at 3400K. As in the case of the cluster, we see that the distribution for the oxygen atoms is slightly wider than the one for the silicon atoms. Furthermore we note also here, that the latter distribution shows a small peak close to the two surfaces, thus signaling the presence of an excess of silicon just below the surface.

The curves shown in Fig. 5 are for $T = 3000$. If the temperature is increased, the height of the flat region at intermediate and small values of r does not change, which is in agreement with the fact that the bulk density of silica is only a weak function of temperature [47], a property that is reproduced well by the present model [40,42]. However, the density profile very close to the surface does depend on temperature in that with increasing temperature the height of the excess peak diminishes and the final decay to zero at large distances becomes less steep. This effect is demonstrated for the film geometry in Fig. 6, where we show the distribution of the total density for three different temperatures (top three curves). This behavior can easily be understood by recalling that at high temperatures the cluster has many small thin arms that contribute to the density also at large distances (see Fig. 1) and hence make the surface less well defined. Since these results for the surface of the clusters and the ones of the films are so similar, and this is the case also for many other ones [39], we will in the following not discuss the latter ones anymore.

A quantity that gives information on the structure on a more microscopic level than the density profile is the (partial) radial distribution function $g_{\alpha\beta}(r)$ [52], which gives the probability of finding an atom of type α at a distance r from an atom of type β , normalized by the phase space factor. In a infinite system (or one with periodic boundary conditions), this factor is just $4\pi r^2$. For an inhomogeneous system this factor depends on the position of atom α and the resulting expression is somewhat cumbersome, but simple to derive. Therefore we refer the interested reader to Ref. [39] for more details on this. In Fig. 7 we show the resulting $g_{\alpha\beta}(r)$ for the largest system at $T = 3000$ K. In each panel two curves are shown: The solid ones correspond to the $g_{\alpha\beta}$ if one of the atoms is in the surface shell (shell 3). The dashed line is for the atoms that are in the interior of the cluster (shell 1). We mention that within the accuracy of our data the curves of shell 1 are identical to the ones of the bulk [42]. This shows that with respect to this observable the interior of the cluster is equivalent to the bulk.

From the figure we recognize that the $g_{\text{SiO}}(r)$ in shell 1 and shell 3 are quite similar. In particular the first nearest neighbor peaks are almost identical, which shows that the surface does not change the nearest neighbor distance in Si-O. This can be understood by recalling that this type of bond is very strong and hence it does not depend on the environment. The second nearest neighbor peak of g_{SiO} is, however, a bit broader than the one in the bulk, which shows that on the surface the system is more heterogeneous than inside. Also the distribution $g_{\text{OO}}(r)$ in shell 3 is quite similar to the one in shell 1, although in this correlation function also differences in the first peak are observed in that on the surface the peak is higher and broader. The largest differences are found in $g_{\text{SiSi}}(r)$, where we see that around 2.5\AA a small shoulder is observed in the curve for the surface. This means that in this shell a new length scale exists, the origin of which will below be shown to be two-membered rings, i.e. a structural unit which is not found in the bulk [40,53]. Finally we mention that we have also calculated the three partial structure factors for the clusters and found that these functions do not show any unexpected behavior or give new insight into the structure of the

droplets, beyond the one of $g_{\alpha\beta}(r)$.

Further relevant information on the local structure can be obtained from the distribution function of the angle between three neighboring particles. For this we define two particles (of type α and β) to be neighbors if their distance is smaller than the first minimum in $g_{\alpha\beta}(r)$. These minima are at 3.63Å , 2.32Å, and 3.24Å, for the Si-Si, the Si-O, and O-O correlation function, see Fig. 7, and are independent of temperature. Some of the angle distribution function $P_{\alpha\beta\gamma}(\theta)$ are shown in Fig. 8a. These data are for the largest system at $T = 3000\text{K}$, and we have found that for the smaller systems the results are very similar. Again we show for each distribution two curves: One for the innermost shell and one for the surface. (Also for this observable the distributions for the interior of the cluster is essentially identical to the one of the bulk.) In contrast to the quantities investigated so far, we see in this observable a very strong difference between the structure in the bulk and the one close to the surface. E.g. the main peaks in P_{SiSiSi} and in P_{SiOsi} for the surface are shifted by about 10° to smaller angles and have become broader. More important, the latter distribution shows now a second peak around 100° , a feature which is not present at all in the bulk. A similar new feature is found in P_{OSiO} , where around 80° a shoulder is observed which is not present in the bulk. Although P_{SiSiSi} shows a secondary peak also in the bulk, its amplitude is much larger in the surface layer.

In Fig. 8b and c we show the temperature dependence of the distribution function P_{SiSiSi} for shell 1 and shell 3, respectively. From panel (b) we see that the secondary peak around 60° mentioned above shows a strong temperature dependence in that its amplitude decreases rapidly with decreasing temperature. In Ref. [40] it was shown that (in the bulk) even at temperature zero a small peak at this angle is observed, but that its amplitude decreases if the cooling rate with which the sample is quenched to low temperatures decreases. Thus those results are in agreement with the present ones. For the case of the surface, the temperature dependence of the amplitude of the secondary peak is much weaker, see panel (c). Thus it is reasonable to assume that this structural feature will be present even at low temperatures, in contrast to the peak in the bulk. A qualitatively similar behavior is found for the secondary peak in P_{SiOsi} . Thus we conclude that the surface has structural elements that are present in the bulk only at high temperatures, whereas on the surface they are found at all temperatures. These results are in qualitative agreement with the (less detailed) studies of Garofalini on these distributions [26].

In order to find out the nature of these structural elements we investigated the distribution of the length of the “rings” in the network. For this we define a ring as follows: Start from any silicon atom and pick two of its nearest neighboring oxygen atoms (neighbors are defined again by means of the minimum in the radial distribution function). Find the *shortest* consecutive sequence of Si-O elements that connect these two oxygen atoms. In this way we have constructed a closed loop of Si-O segments and the length of the ring is defined as the number of silicon atoms in this loop. Note that if an oxygen is attached only to one Si atom, i.e. a non-bridging oxygen, we define this length to be 1. The interest in these rings stem from the fact that they give information on the structure on intermediate distances. Also, since the connectivity of silicon atoms can (indirectly) be studied in NMR experiments (see, e.g., Ref. [54] and references therein), they are not only of theoretical, but also of experimental relevance, thus justifying the investigations on them done in the past [40,53].

In Fig. 9 we show the distribution function $P(n)$, i.e. the probability that a ring has length n . The data is for the largest system and we show the distribution for the interior and the surface at two temperatures. (A ring belongs to the surface if at least one silicon atom is in shell 3.) From the graph we see that the most probable length of a ring is 5 or 6, a result that can be understood by recalling that on the local length scale the structure of the melt at zero pressure will be very similar to the one of β -cristobalite [55], a crystalline form of SiO_2 that has only 6 membered rings. Note that the whole distribution for the surface is shifted a bit to smaller values of n . This effect can be understood by realizing that if an atom is close to the surface it is more difficult for it to be part of a large ring, due to entropic reasons.

At high temperatures, $T = 4700\text{K}$, one sees that also the above mentioned dangling bonds, $n = 1$, are quite frequent, in particular at the surface. This is in qualitative agreement with the configuration snapshot of Fig 1. The number of the mentioned dangling bonds depends strongly on temperature in that a change of T from 4700K to 3000K gives rise to a decrease by a factor of 4-5 in the case of the surface and in the interior they practically vanish completely. For the two-membered rings the situation is different. Although in the interior the change of temperature leads again to a very strong reduction of their frequency, their number decreases only slightly in the case of the surface. Also rings of length three are, at the lower temperature, roughly three times more frequent on the surface than in the bulk. Thus we conclude that close to the surface there is a substantial fraction of very short rings. Due to their shortness, the angles occurring in such rings are relatively small, which explains our findings on the distribution of the bond-bond angles, Fig. 8, that in the outermost shell peaks at relatively small angles appear. These results are in qualitative agreement with the ones found earlier by Feuston and Garofalini [30], although the relative intensities are quite different.

We now investigate the question whether the presence of a surface changes only the relative frequency with which a ring of a given length appears, or whether also the properties of the ring changes. In Fig. 10 we show the distribution of the Si-O-Si angles occurring in a ring with length $n = 2$ and $n = 3$. The solid and dashed lines are for the rings in the outermost shell and the interior of the cluster, respectively. We see that the angle for two-membered rings has a peak around 95° . This angle corresponds to the location of the secondary peak that we found in the total distribution function in Fig. 8a. Thus we can conclude that this peak stems from two-membered rings. (Note that in Fig. 8a the curve for the interior was very close to zero around 95° . The reason why we see now in Fig. 10 nevertheless a peak is that *a few* two-membered rings are present anyway. Since there are only a few of short rings, the curves for the bulk are quite noisy.) From Fig. 10 we see that within the accuracy of our data the distribution of the angles is the same in the interior and the surface of the system. The same is found for the angle O-Si-O as well as for longer rings. Therefore we conclude that the structure of the rings is independent of their location and the difference between the surface and the interior is only the frequency of the various rings.

In Tab. I we give the geometry of the two-membered rings as found in the present simulation and compare it with values from another classical simulation and quantum mechanical calculations. From this list we see that although our simulation underestimates and overestimates the O-Si-O and Si-O-Si angles, respectively, as obtained by the *ab initio* calculations

by around $7-8^\circ$, the various distances are reproduced well. Regarding the discrepancies in the angles it has to be realized that the quantum mechanical calculations have been done for very small clusters of SiO_2 , thus structures that were not part of a larger network. That such a network can have a significant effect on the form of the two-membered rings can be inferred from the last line in the table where we give the geometry of so-called “silica-w”, a synthetic polymorph of SiO_2 which contains only chains of two-membered rings. We see that in this material the geometry of these rings is very different from the ones found in the small molecules, thus showing the importance of the surrounding.

In order to get a better understanding on the geometry of the surface we show in Fig. 11 a snapshot of the largest system at 3000K. All atoms are shown that have a distance from the center that is larger than 20\AA . Since for this system size the typical radius of the cluster is 26\AA , we thus show the top $6-7\text{\AA}$, i.e. basically the shell that we defined to be the surface. The dark and light gray atoms are the silicon and oxygens, respectively. Marked in black are the two-membered rings. (Note that for the sake of a better representation we show only the upper half of the cluster.) From the figure we recognize that the rings do not show any tendency to cluster, but rather seem to stay apart from each other. The reason for this is likely that a region with such a ring has a relatively high stress and thus bringing two such rings close together is energetically rather unfavorable. We also mention that for the largest system we find on the order of 50 two-membered rings on the surface. With a surface area of around 8500\AA^2 this value thus corresponds to an average density of 0.6 rings per nm^2 . This value is in good agreement with experimental data, which varies between 0.1-0.4 rings per nm^2 [12,15,14] and other simulations which give values between 0.13-3.0 rings per nm^2 [31,35,28,30,23]. Note, however, that in Fig. 9 we see that the number of these rings decreases slowly with temperature. Thus it can be expected that the present value for the density of rings decreases if one would be able to equilibrate the system at even lower temperatures.

Having now discussed the static properties of the clusters we turn in the final part of this section to the dynamics of this system. One of the simplest dynamical quantities for a liquid is the mean-squared displacement (MSD) of a tagged particle i , $\langle r^2(t) \rangle = \langle |\mathbf{r}_i(t) - \mathbf{r}_i(0)|^2 \rangle$, where $\mathbf{r}_i(t)$ is the location on the particle at time t . In Fig. 12 we show the time dependence of $\langle r^2(t) \rangle$ for the silicon atoms at 3000K. (The curves for the oxygen atoms look qualitatively the same.) Three curves are shown: the ones in which at time zero the atoms were in shell 1 or shell 3, and the curve for the bulk from Ref. [42]. Before we discuss the three curves let us briefly comment on the various time regimes of the dynamics. At very short times, $t \leq 0.02\text{ps}$, the particles move just ballistically, $\langle r^2(t) \rangle \propto t^2$, since their motion is not affected by the presence of all the other particles. At times around 0.1ps the particles collide with their neighbors and they rattle around in the cage formed by these neighbors. Hence the MSD is almost constant for a around two decades in time. Only at much longer times the particles are able to escape this cage and to become diffusive, i.e. $\langle r^2(t) \rangle \propto t$. This sequence is the general behavior found for the MSD in a liquid with glassy dynamics [57].

From the figure we see that at short times, i.e. in the ballistic regime, the dynamics of the atoms is independent of the shell, since in this time window the environment does not yet affect the motion of the particles. The first differences between the first and third shell are noticeable for $t \geq 0.04\text{ps}$, in that the MSD of the particles at the surface is larger than the one of the particles in the interior. At these times the motion of the particles has

still a strong vibrational character [42] and thus we conclude that the cages seen by the particles are larger close to the surface than in the interior of the cluster. This result is very reasonable since we have seen above that the atoms close to the surface have more defects and hence it can be expected that the size of their cage is larger. Apart from the larger size of the cages, i.e. a higher value of the plateau in the MSD, the dynamics of the particles in the surface shell seems to be quite similar to the one in the bulk, at least as can be inferred from this observable (see, however, the vibrational spectrum discussed below). Furthermore one can conclude from the graph that the dynamics of the particles inside the cluster is very similar to the one in the bulk, since only in the plateau regime small differences can be observed.

We also mention that we have also calculated the components of the MSD that are parallel and perpendicular to the surface. We have found that at low temperatures the radial component for silicon (multiplied by 1.5 to correct for the trivial geometric factor) is slightly larger than its parallel component. However, this effect was only small, $O(20\%)$, and observable only in the time regime in which the MSD is almost constant. This shows that the dynamics of the particles is almost isotropic. The small difference can be understood by recalling that on the surface the particles are not caged very efficiently, since there are no caging particles towards the vacuum.

Finally we remark that the largest values of $\langle r^2(t) \rangle$ is around 22\AA^2 , which means that on average a particle has moved a distance around 5\AA . Thus if at time zero an atom was in a certain shell it will usually not be able to leave this shell within the time span of the simulation. However, for very long times the system is of course ergodic and thus the MSD becomes independent of the shell in which the tagged particle started in. In fact, from the figure one already sees that for times larger than a few hundred ps the curve for shell 3 starts to approach the one for shell 1.

From the MSD at long times and the Einstein relation one can immediately calculate the diffusion constant D : $D = \lim_{t \rightarrow \infty} \langle r^2(t) \rangle / 6t$. (Here we have taken the average only over the particles of shell 1.) For the case of silicon, the resulting values of D are shown in Fig. 13 in an Arrhenius plot. The data for oxygen look qualitatively similar [39]. The different curves correspond to the various system sizes and in addition we have also included the curve from the bulk [42]. From the plot one recognizes immediately that the relaxation dynamics of the particles in the finite clusters is faster than the one in the bulk. However, for the largest system this difference is only very small. We also mention that for a strong glass former like silica [58], one might expect that the temperature dependence of D is an Arrhenius law. Instead we find that *at intermediate and high* temperatures, quite strong deviation from this law are present. In Ref. [42] it was argued that at these high temperatures the dynamics of the system is qualitatively different from the one at lower temperatures since the effects described by the so-called mode-coupling theory of the glass transition become important [59]. Only at low temperatures, which for silica are presently just barely accessible in a computer simulation, does the dynamics cross over to an activated one and thus the temperature dependence of the transport coefficients become an Arrhenius law. We stress, however, that the present model of silica seems indeed to be able to reproduce reliably the dynamics at low temperatures, since, e.g., quantities like the activation energy of D for Si and O, as well as the one of the viscosity are reproduced well [42].

In order to show to what extent the relaxation dynamics depends on the shell, we plot in

Fig. 14 the ratio of the diffusion constant For the particles on the surface and in the interior. From this figure we recognize that at all temperatures investigated this ratio is significantly larger than one and increases with decreasing temperature. For the larger system, filled symbols, this ratio is independent of the type of particle. (Although for the intermediate system the ratio for Si and O are not the same, this is probably due to the relatively large error for the Si data for this value of N .) Thus we conclude that with decreasing temperature the motion of the particles on the surface decouples from the ones of the particles in the interior.

In order to understand better the reason for this decoupling it is useful to investigate the diffusion process a bit closer. For this we define the function $P_B(t)$, the probability that a bond between a silicon and a neighboring oxygen atom that is present at time zero is also present at time t . In the past it has been found that in the bulk the shape of $P_B(t)$ is independent of temperature and that therefore it is possible to define a typical life-time of a bond, τ_B , by $P_B(\tau) = e^{-1}$ [42]. In Fig. 15 we plot the product $\tau_B D_\alpha$ for bonds in the surface and in the interior. In agreement with the results from the bulk we find that for shell 1 this product is independent of T for the case of oxygen, which shows that the breaking of the bond is the elementary diffusion step for the oxygen atoms. This is not the case for the atoms in the surface, since for silicon as well as oxygen the product depends on temperature in that it decreases with decreasing T . Thus we conclude that the breaking of a Si-O bond is not the elementary step for the diffusion at the surface. One possibility for the explanation of this trend is, i.e., that with decreasing temperature the number of dangling oxygens is decreasing (see Fig. 9) and hence the number of more mobile atoms is decreasing. We also mention that Litton and Garofalini have presented results from simulations in which they found that the enhanced diffusivity of the particles near the surface is related to the fact that these atoms can make larger jumps [32]. However, these results were obtained at a relatively high temperature, i.e. in a regime where the surface still has many arms sticking out into the vacuum (see Fig. 1a). Since these structures are not present at the lower temperatures it should not be expected that this type of reasoning is applicable also at low temperatures.

It is also instructive to investigate the typical life-time of a particular defect. For oxygen, the vast majority of defects are one and three coordinated atoms (i.e. the coordination number is $z = 1$ or $z = 3$) and thus we will concentrate in the following on these type of defects. In Fig. 16a we show for two temperatures the probability that a defect that was present at time zero exists also at time t . From this graph we recognize that the typical life-time for a defect of type $z = 3$, dashed-dotted curves, is much shorter, 0.1-1.0ps, than the one of a bond, dashed curves. Furthermore we see that the temperature dependence of this life-time is relatively weak, since a change of T from 4700K to 3000K gives rise to an increase of only a factor of 2-3, whereas the curves for $P_B(t)$ are shifted by around a factor of 100. The situation is very different for defects of type $z = 1$, i.e. the dangling bonds (solid curves). Here we see that the curve shows a strong temperature dependence, although it is not quite as strong as the one for $P_B(t)$.

The curves shown in Fig. 16a are for the largest cluster, taking into account *all* the atoms. In Fig. 16b we now study the dependence of these probabilities on the shell in which the defect is for the case $T = 3000\text{K}$. From this graph we recognize that the life-time of a $z = 3$ defect is very short in the bulk as well as on the surface (dashed curves). (Note that the statistics of these two curves is very poor, since at $T = 3000\text{K}$ there are only very

few defects of this type.) For the dangling bonds, however, there is a big difference in the survival probability (solid curves). In the interior the defects are annihilated very quickly, i.e. within 1ps, whereas on the surface they survive for a long time. Thus we conclude that the large annihilation time for the dangling bonds in Fig. 16a is due to the fact that on the surface these defects survive for a long time. The reason for this large difference is probably that from an energetic point of view it is *in the bulk* very unfavorable to have a defect and thus it is very unstable. The situation is different on the surface, since a dangling bond that sticks out from the surface does not cost too much energy and thus can survive for a long time. Finally we mention that we found that also the defect coordinated silicon atoms, mainly $z = 3$ or $z = 5$, stay in this state only for a relatively short time, i.e. less than one ps. The only exception are the three-fold coordinated Si-atoms at the surface which can stay in that state for up to 2 ps [39]. But as can be seen from Fig 16b, even this time is much shorter than the typical life-time of a dangling bond at the surface.

The final quantity we investigate is $g(\nu)$, the vibrational density of state (DOS). For this we quenched a liquid sample from 3000K rapidly to $T = 300\text{K}$ (100.000 steps = 163 ps) and, after annealing the sample a bit, calculated $g(\nu)$ via the Fourier transform of the velocity autocorrelation function [60]:

$$g(\nu) = \frac{1}{Nk_B T} \sum_j m_j \int_{-\infty}^{\infty} dt \exp(i2\pi\nu t) \langle \vec{v}_j(t) \vec{v}_j(0) \rangle \quad . \quad (4)$$

The Fourier transform was calculated by making use of the Wiener-Khinchin theorem [61]. Note that this way to calculate the DOS allows to decompose $g(\nu)$ into the individual contributions from the different atoms, and hence into the atoms in the different shells. In Fig. 17a we show the so obtained DOS as obtained by considering only the atoms in the interior, or in the surface layer (thin and bold solid curves, respectively). We see that the two distributions are quite similar and also quite close to the one of the bulk [41]. The main difference is that in the curves for the cluster the double peak at high frequencies is not separated as well as in the bulk and that also the minimum around 28THz is not so pronounced. (We remind the reader that the origin of these two peaks is an intra-tetrahedral motion of the atoms [62,63].) Since all three curves are quite similar one might conclude that the presence of the surface does not affect significantly the DOS. That this conclusion is incorrect is shown in Fig. 17b, where we show the contributions to the DOS from the silicon and oxygen atoms in shell 1 and shell 3. From the graph we recognize that the vibrational spectrum for the oxygen atoms is indeed almost independent of the shell (dashed lines). In particular we see that the location and the intensity of the two peaks at high frequency is very similar in the two distributions. For the silicon atoms, however, we find a significant difference between the two DOS. In the $g(\nu)$ for the surface the two peak at high frequencies are shifted from 32.0 and 35.2THz to 30.4 and 32.9THz, respectively. Since these peaks stem from the motion of the atoms within one tetrahedron it is quite reasonable to find that close to the surface this type of motion has a lower frequency, since the atoms are less constrained. A further large change in the DOS is found around 22.2THz, where on the surface the peak is less pronounced. Such a decrease has also been found in the simulations by Beckers and de Leeuw of porous silica [36], i.e. a system with a large surface area. Since in that simulation the silica potential proposed by Vashishta *et al.* was used [45], we conclude that the described decrease is not an artifact of the BKS potential but a real dynamical feature

of the silica surface. Experimental infrared studies have shown that the presence of two-membered rings gives rise to bands at 26.6 and 27.2THz [10,12,15]. Although this frequency is reproduced reasonably well by density functional approaches [23] which underestimates the two frequencies by 5%, the classical simulation have so far not been able to get a good agreement with the experimental results. Although we find a small peak at around 28THz, see Fig. 17b, it is presently not clear whether it does indeed correspond to the motion of the atoms in two-membered rings.

IV. SUMMARY AND DISCUSSION

The goal of this paper was to investigate the static and dynamical properties of the surface of amorphous silica *in equilibrium*. For this we did molecular dynamics computer simulations, using a potential that in the past has been shown to be very reliable in the bulk. Two types of geometries were investigated: Finite clusters with different numbers of atoms (and hence surface area) and a thin film. Although the results discussed in the present paper referred almost exclusively to the clusters, we have found that the surface properties of the thin film are, within the accuracy of our data, the same as the ones for the clusters. Hence we conclude that the curvature of the surface in the cluster geometry is basically irrelevant.

We have found that in the temperature range investigated the shape of the clusters does not depend on T . From the size dependence of the potential energy per particle we estimate that the surface energy of the system is around 1 N/m, a result which is in rough agreement with the experimental value for the surface tension. In agreement with previous simulations [32] we find an enrichment of oxygen close to the surface. The reason for this effect is that in this way the number of energetically frustrated bonds is minimized. The study of the partial radial distribution functions $g_{\alpha\beta}(r)$ as well as of the distribution functions for the bond-bond angles shows that at the surface there are structural units that are not existent in the bulk (or rather they occur with an extremely small probability) and which should be present also at low temperatures. By calculating $P(n)$, the probability that a ring has length n , we show that short rings are much more frequent on the surface than in the bulk. By determining the structural properties of these short rings we demonstrate that the mentioned anomalous features in the $g_{\alpha\beta}(r)$ and the bond-bond angle distribution functions are closely related to these short rings. The average density of the two-membered rings is 0.6 rings/nm², in reasonable good agreement with experimental estimates. Also the geometry of these two-membered rings is in good agreement with *ab initio* simulations. Thus we come to the conclusion that the BKS-potential used here is indeed able to give a realistic description not only of vitreous bulk silica but also of the surface of amorphous silica. This conclusion is at odds with the one of Ref. [23] where it is stated that this model gives rise to too many over and undercoordinated surface atoms. Although the BKS-potential is certainly far from being perfect the present work shows that if the surface is properly relaxed the resulting structure is very reasonable.

We have also investigated the dynamics of the system. For times larger than the ballistic regime we find that the MSD for the atoms at the surface is larger than the one in the interior. Thus we conclude that at the surface the cage of the atoms is larger than the one in the bulk. The cluster-averaged diffusion constant depends significantly on the size of the cluster and this dependency becomes stronger with decreasing temperature. In order

to study the diffusion mechanism in more detail we have determined the probability that a oxygen defect which is present at time zero is also present at time t . We find that an oxygen atom that is three-fold coordinated stays in that state for less than a ps (whether or not the defect is at the surface). In contrast to this the singly coordinated oxygen atoms, i.e. the dangling bonds, stay in that state for a very long time (100ps at 3000K) if the defect is at the surface, whereas it disappears already after 1ps if it is in the bulk. Thus this shows that on the surface the dangling bonds are very stable structures, at least at these high temperatures.

Finally we have also determined the vibrational density of states (DOS). We find that the total DOS for the whole cluster is quite similar to the one of the bulk. However, if the total DOS is decomposed into the parts corresponding to the silicon and oxygen atoms, we find that the DOS for the silicon atoms close to the surface is quite different from the one in the bulk. No such difference is found in the oxygen atoms. Thus we conclude that the presence of the surface can be seen also in the vibrational dynamics of the ions.

In summary we thus conclude that the BKS model seems to be capable to give also a very reasonably description of the surface of amorphous silica. Unfortunately not much *structural* information on this type of surface is presently known from experiments and hence it is difficult to judge the quality of the present results on a *quantitative* level. However, using new microscopic techniques like an STM or an AFM it should be possible to obtain in the near future experimental data [16–18]. Furthermore it will also be valuable to compare the present results with the ones obtained with a method that is more accurate, such as the one proposed by Car and Parrinello [64]. Although the time window that can be accessed by this method is more than thousand times smaller than the classical simulations of the present work, such a comparison will nevertheless give useful information on the reliability of the BKS-potential in the presences of a surface.

Acknowledgement: We gratefully acknowledge the financial support by the SCHOTT Glaswerke Fond and the DFG under SFB 262. Part of this work was done at the NIC in Jülich.

REFERENCES

- [1] See, e.g., articles in the proceeding of the *Third International Discussion Meeting on Relaxation in Complex Systems*, J. Non-Cryst. Solids **235-237** (1998).
- [2] Proceedings of *Unifying concepts in glass physics*, J. Phys.: Condens. Matter **12**, 6295 (2000).
- [3] C. G. Pantano, Rev. Solid. State Sci. **3**, 379 (1989).
- [4] Proceedings of *International Workshop on Dynamics in Confinement*, Journal de Physique IV **10**, Proceedings Pr7 (2000).
- [5] A. P. Legrand, *The Surface Properties of Silica* (Wiley, New York, 1998).
- [6] R. K. Iler, *The Chemistry of Silica* (Wiley, New York, 1979).
- [7] C. R. Helms and B. D. Deal, *The Physics and Chemistry of SiO₂ and the Si-SiO₂ interface*, Vol. 2, (Plenum, New York, 1993).
- [8] J. F. Conley and P. M. Lenahan, Appl. Phys. Lett. **62**, 40 (1993).
- [9] E. E. Stahlbush, A. H. Edwards, D. L. Griscom, and B. J. Mrstik, J. Appl. Phys. **73**, 658 (1993).
- [10] B. A. Morrow and I. A. Cody, J. Phys. Chem. **80**, 1995 (1976).
- [11] T. A. Michalske and B. C. Bunker, J. Appl. Phys. **56**, 2686 (1984).
- [12] B. C. Bunker, D. M. Haaland, K. J. Ward, T. A. Michalske, W. L. Smith, J. S. Binkley, C. F. Melius, and C. A. Balfe, Surf. Sci. **210**, 406 (1989).
- [13] L. H. Dubois and B. R. Zegarski, J. Phys. Chem. **97**, 1665 (1993).
- [14] L. H. Dubois and B. R. Zegarski, J. Am. Chem. Soc. **115**, 1190 (1993).
- [15] A. Grabbe, T. A. Michalske, and W. L. Smith, J. Phys. Chem. **99**, 4648 (1995).
- [16] E. Rädlein, R. Ambos, and G. H. Frischat, Fres. J. Anal. Chem. **353**, 413 (1995).
- [17] W. Raberg and K. Wandelt, Appl. Phys. A **66**, S1143 (1998).
- [18] P. K. Gupta, D. Inniss, C. R. Kurkjian, and Q. Zhong, J. Non-Crys. Solids **262**, 200 (2000).
- [19] C. A. Murray and T. J. Greytak, Phys. Rev. B **20**, 3368 (1979); D. M. Krol and J. G. van Lierop, J. Non-Crys. Solids **68**, 163 (1984); C. J. Brinker, D. R. Tallant, E. P. Roth, and C.S. Ashley, J. Non-Crys. Solids **82**, 117 (1984); L. T. Zhuravlev, Langmuir **3**, 316 (1987); B. C. Bunker, D. M. Haaland, T. A. Michalske, and W. L. Smith, Surf. Sci. **222**, 95 (1989); B. A. Morrow and A. J. McFarlan, J. Non-Crys. Solids **120**, 61 (1990); I.-S. Chuang, D. R. Kinney, C. E. Bronnimann, R. C. Zeigler, and G. F. Maciel, J. Phys. Chem. **96**, 4027 (1992); D. R. Kinney, I.-S. Chuang, and G. F. Maciel, J. Am. Chem. Soc. **115**, 6786 (1993); I.-S. Chuang, and G. F. Maciel, J. Am. Chem. Soc. **118**, 401 (1996).
- [20] F. Kudo and S. Nagase, J. Am. Chem. Soc. **107**, 2589 (1984).
- [21] M. O’Keeffe and G. V. Gibbs, J. Phys. Chem. **89**, 4574 (1985).
- [22] D. R. Hammann, Phys. Rev. B **55**, 14784 (1997).
- [23] D. Ceresoli, M. Bernasconi, S. Iarlori, M. Parrinello, and E. Tosatti, Phys. Rev. Lett. **84**, 3887 (2000).
- [24] N. Lopez, M. Vitiello, F. Illas, and G. Pacchioni, J. Non-Crys. Solids **271**, 56 (2000).
- [25] M. Vitiello, N. Lopez, F. Illas, and G. Pacchioni, J. Phys. Chem. A **104**, 4674 (2000); T. Uchino and T. Yoko, Phys. Rev. B **58**, 5322 (1998); T. Uchino and T. Yoko, J. Chem. Phys. **108**, 8130 (1998).
- [26] S. H. Garofalini, J. Chem. Phys. **78**, 2069 (1983).

- [27] S. H. Garofalini and S. Conover, *J. Non-Crys. Solids* **74**, 171 (1985).
- [28] S. M. Levine and S. H. Garofalini, *J. Chem. Phys.* **86**, 2997 (1987).
- [29] B. P. Feuston and S. H. Garofalini, *J. Chem. Phys.* **89**, 5818 (1988).
- [30] B. P. Feuston and S. H. Garofalini, *J. Chem. Phys.* **91**, 564 (1989).
- [31] B. P. Feuston and S. H. Garofalini, *J. Appl. Phys.* **68**, 4830 (1990).
- [32] D. A. Litton and S. H. Garofalini, *J. Non-Crys. Solids* **217**, 250 (1997).
- [33] V. A. Bakaev, *Phys. Rev. B* **60**, 10723 (1999).
- [34] N. Capron, A. Lagraa, S. Carniato, and G. Boureau, *J. Non-Crys. Solids* **216**, 10 (1997).
- [35] V. A. Bakaev and W. A. Steele, *J. Chem. Phys.* **111**, 9803 (1999).
- [36] J. V. L. Beckers and S. W. de Leeuw, *J. Non-Crys. Solids* **261**, 87 (2000).
- [37] V. I. Bogillo, L. S. Pirnach, and A. Dabrowski, *Langmuir* **13**, 928 (1997); V. A. Bakaev, W. A. Steele, T. I. Bakaeva, and C. G. Pantano, *J. Chem. Phys.* **111**, 9813 (1999); M. M. Branda, R. A. Montani, and N. J. Castellani, *Surf. Sci.* **446**, L89 (2000); M. Rarivomanantsoa, P. Jund, and R. Jullien, preprint 2000.
- [38] B. W. H. van Beest, G. J. Kramer, and R. A. van Santen, *Phys. Rev. Lett.* **64**, 1955 (1990).
- [39] A. Roder, PhD Thesis (University of Mainz, 2000).
- [40] K. Vollmayr, W. Kob, and K. Binder, *Phys. Rev. B* **54**, 15808 (1996).
- [41] J. Horbach, W. Kob, and K. Binder, *J. Phys. Chem. B* **103**, 4104 (1999).
- [42] J. Horbach and W. Kob, *Phys. Rev. B* **60**, 3169 (1999).
- [43] J. Horbach, W. Kob, and K. Binder, preprint cond-mat/9910445.
- [44] K. Vollmayr and W. Kob, *Ber. Bunsenges. Phys. Chemie* **100**, 1399 (1996); T. Koslowski, W. Kob, and K. Vollmayr, *Phys. Rev. B* **56**, 9469 (1997); S. N. Taraskin and S. R. Elliott, *Europhys. Lett.* **39**, 37 (1997); S. N. Taraskin and S. R. Elliott, *Phys. Rev. B* **56**, 8605 (1997); S. N. Taraskin and S. R. Elliott, *Phys. Rev. B* **61**, 12017 (2000); J. Horbach, W. Kob, and K. Binder, *J. Non-Cryst. Solids* **235–237**, 320 (1998); J. Horbach, W. Kob, and K. Binder, *Phil. Mag. B* **77**, 297 (1998); P. Jund and R. Jullien, *Phys. Rev. B* **59**, 13707 (1999); M. Benoit, S. Ispas, P. Jund, and R. Jullien, *Eur. Phys. J. B* **13**, 631 (2000); J. S. Tse and D. D. Klug, *Phys. Rev. Lett.* **67**, 3559 (1991); J. Chem. Phys. **95**, 9176 (1991); J. S. Tse, D. D. Klug and Y. Le Page, *Phys. Rev. B* **46**, 5933 (1992); *Phys. Rev. Lett.*, **69**, 3647 (1992); J. S. Tse, D. D. Klug and D. C. Allan, *Phys. Rev. B* **51**, 16392 (1995).
- [45] P. Vashishta, R. K. Kalia, and I. Ebbsjö, *Phys. Rev. B* **41**, 12197 (1990).
- [46] For another simulation of SiO₂ clusters see C. Brangian, O. Pilla, and G. Viliani, *Phil. Mag. B* **79**, 1971 (1999).
- [47] O. V. Mazurin, M. V. Streltsina, and T. P. Shvaiko-Shvaikovskaya, *Handbook of Glass Data, Part A: Silica Glass and Binary Silicate Glasses* (Elsevier, Amsterdam, 1983).
- [48] D. E. Parry, *Surf. Sci.* **49**, 433 (1975); *ibid.* **54**, 195 (1976).
- [49] D. M. Heyes, *Phys. Rev. B* **30**, 2182 (1984); *ibid.* **49**, 755 (1994).
- [50] In principle also *single* silicon or oxygen atoms could evaporate. However, in this case the escape velocity is significantly higher, since the Coulomb attraction has to be overcome. Hence this type of escape is less frequent than the one of small neutral fragments.
- [51] J. Jäckle and K. Kawasaki, *J. Phys.: Condens. Matter* **7**, 4351 (1995).
- [52] J.-P. Hansen and I. R. McDonald, *Theory of Simple Liquids* (Academic, London, 1986).
- [53] J. P. Rino, I. Ebbsjö, R. K. Kalia, A. Nakano, and P. Vashishta, *Phys. Rev. B* **47**, 3053

- (1993).
- [54] See, e.g., J. F. Stebbins, *Rev. Mineral.*, **32**, 191 (1995).
 - [55] D. Stöffler and J. Arndt, *Naturwissenschaften* **56**, 100 (1969).
 - [56] A. Weiss and A. Weiss, *Z. Anorg. Allg. Chem.* **276**, 95 (1954).
 - [57] W. Kob, *J. Phys.: Condens. Matter* **11**, R85 (1999).
 - [58] C. A. Angell, in *Relaxation in Complex Systems*, Eds.: K. L. Ngai and G. B. Wright (US Dept. Commerce, Springfield, 1985).
 - [59] W. Götze, p. 287 in *Liquids, Freezing and the Glass Transition* Eds.: J.-P. Hansen, D. Levesque, and J. Zinn-Justin, Les Houches. Session LI, 1989 (North-Holland, Amsterdam, 1991); W. Götze, *J. Phys.: Condens. Matter* **10A**, 1 (1999).
 - [60] M. T. Dove, *Introduction to Lattice Dynamics* (Cambridge University Press, Cambridge, 1993).
 - [61] W. H. Press, B. P. Flannery, S. A. Teukolsky, and W. T. Vetterling, *Numerical Recipes* (Cambridge University Press, Cambridge, 1986).
 - [62] F. L. Galeener, *Phys. Rev. B* **19**, 4292 (1979).
 - [63] A. Pasquarello, J. Sarnthein, and R. Car, *Phys. Rev. B* **57**, 14133 (1998) and references therein.
 - [64] D. Marx and J. Hutter, *Mod. Meth. and Alg. of Quant. Chem.* **1**, 301 (2000).

FIGURES

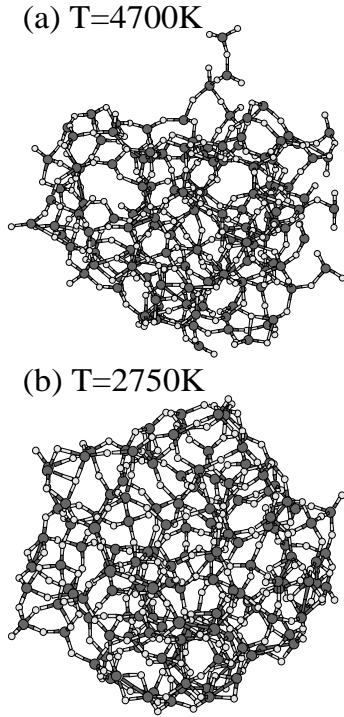


FIG. 1. Snapshot of the system with 432 ions at two different temperatures. The dark and light gray spheres correspond to the silicon and oxygen atoms, respectively.

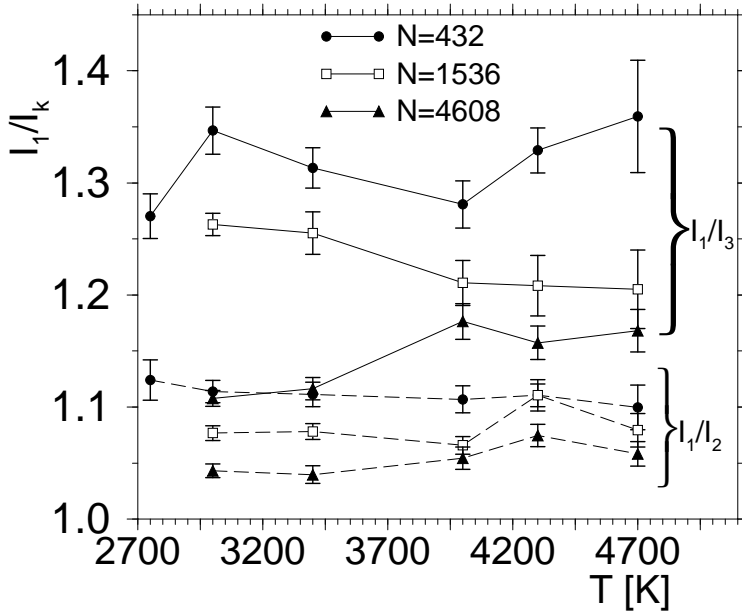


FIG. 2. Temperature dependence of the ratio of the principal moments of inertia, $I_1 \geq I_2 \geq I_3$, for the three system sizes.

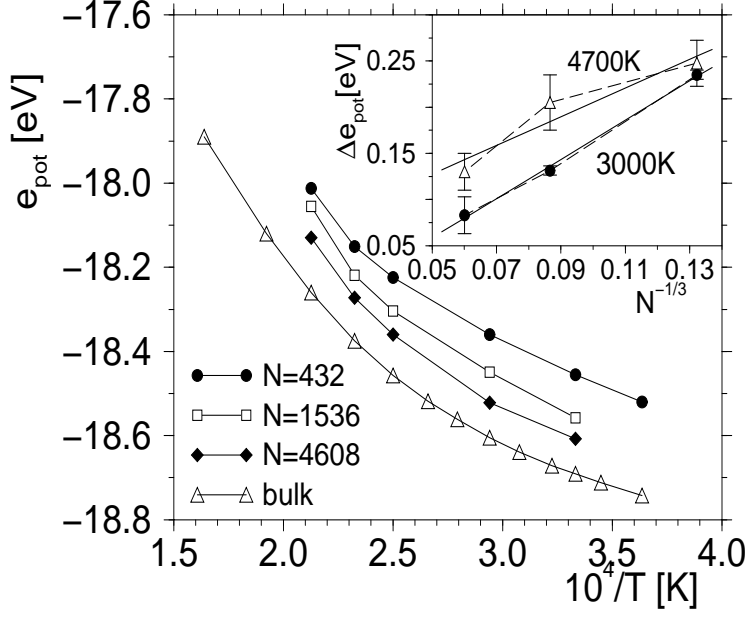


FIG. 3. Temperature dependence of the potential energy per particle for the three system sizes and the bulk from Ref. [42]. Inset: Difference between $e_{\text{pot}}(N)$ and the potential energy in the bulk for two temperatures.

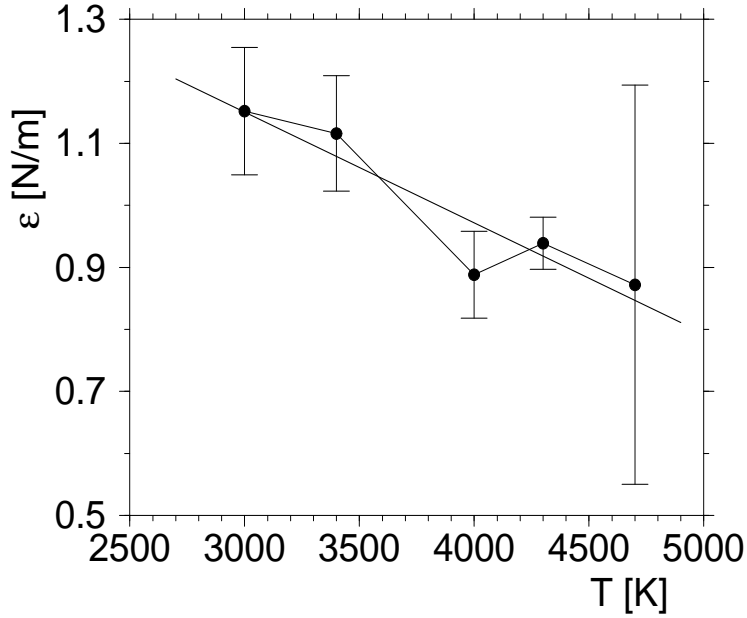


FIG. 4. Temperature dependence of ϵ , the surface energy per unit area. The solid line is a linear fit to the data.

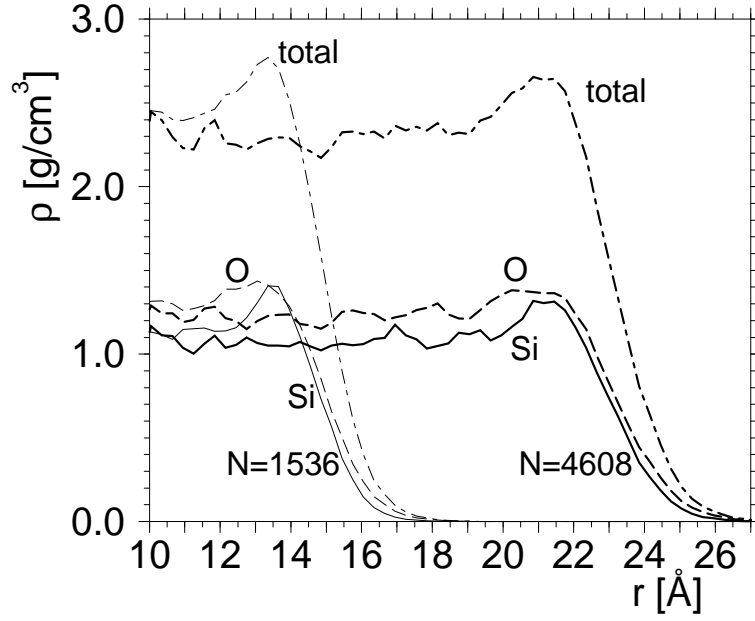


FIG. 5. Density profile for the medium and large cluster (thin and bold curves, respectively). Dashed-dotted lines are for the total density. Solid and dashed lines are for the density of silicon and oxygen, respectively.

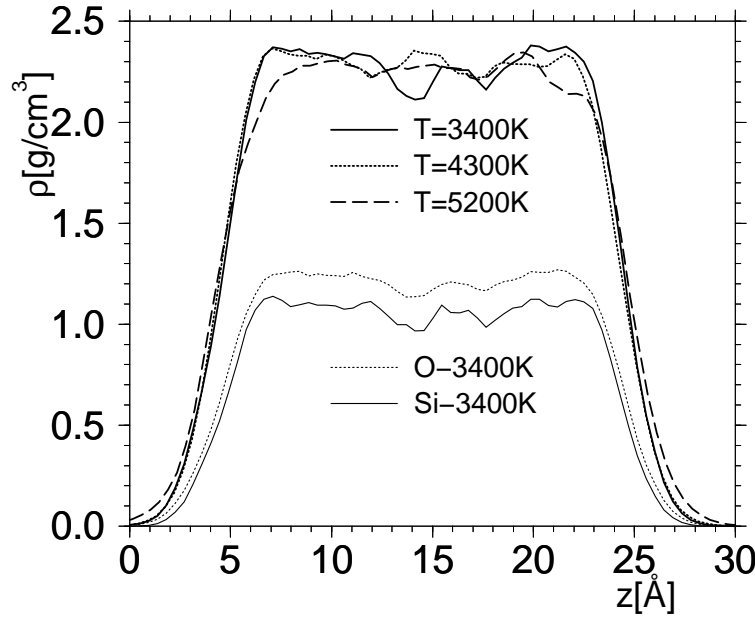


FIG. 6. Density profile for the thin film. The upper three curves are the total mass density at three different temperatures. The lower two curves are the density for the oxygen and silicon atoms at $T = 3400\text{K}$.

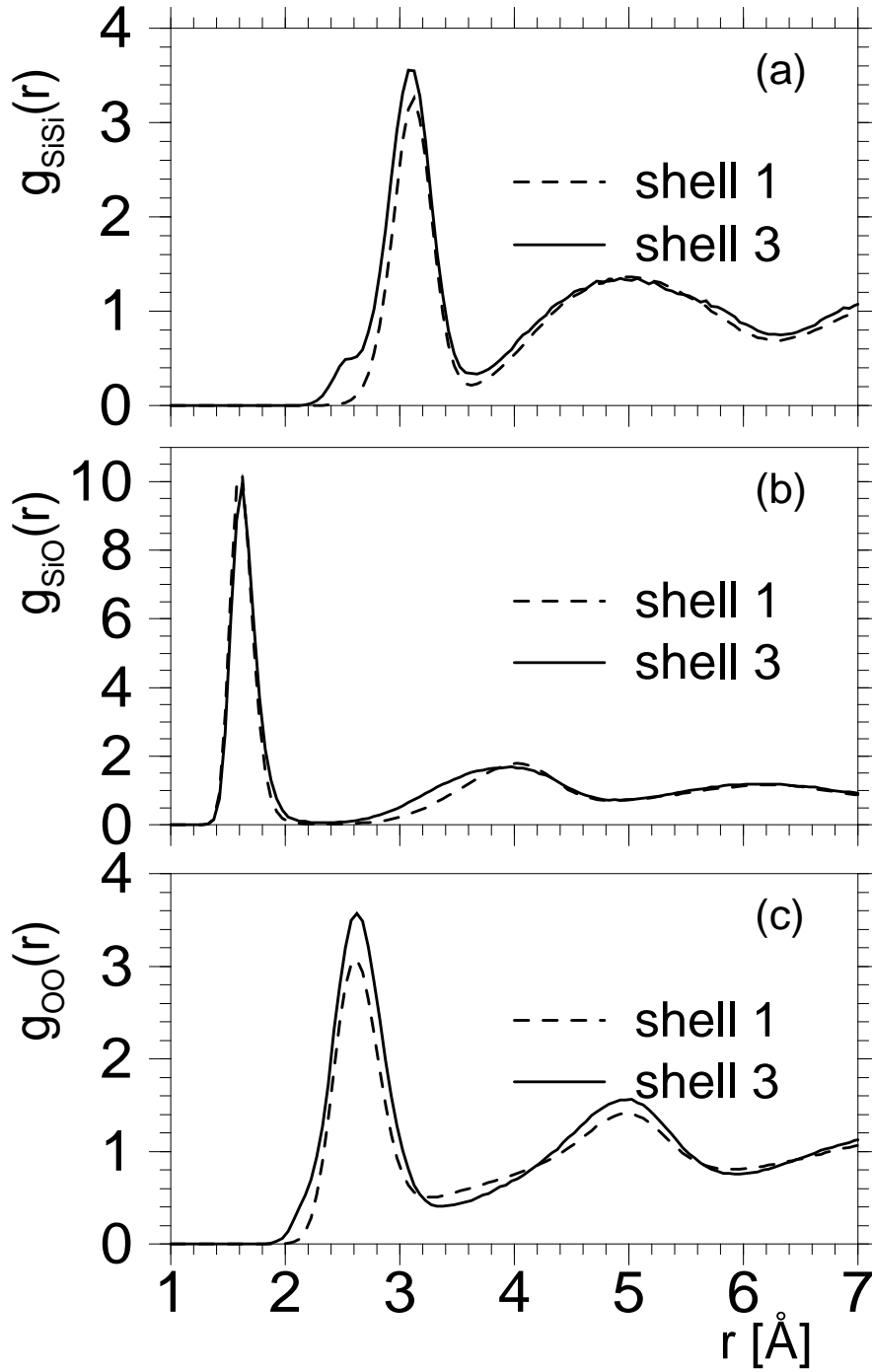


FIG. 7. Partial radial distribution functions $g_{\alpha\beta}(r)$ for the cluster with $N = 4608$ ions at $T = 3000\text{K}$. Shell 1 and 3 correspond to the interior and surface of the cluster, respectively. a) $g_{\text{SiSi}}(r)$, b) $g_{\text{SiO}}(r)$, c) $g_{\text{OO}}(r)$.

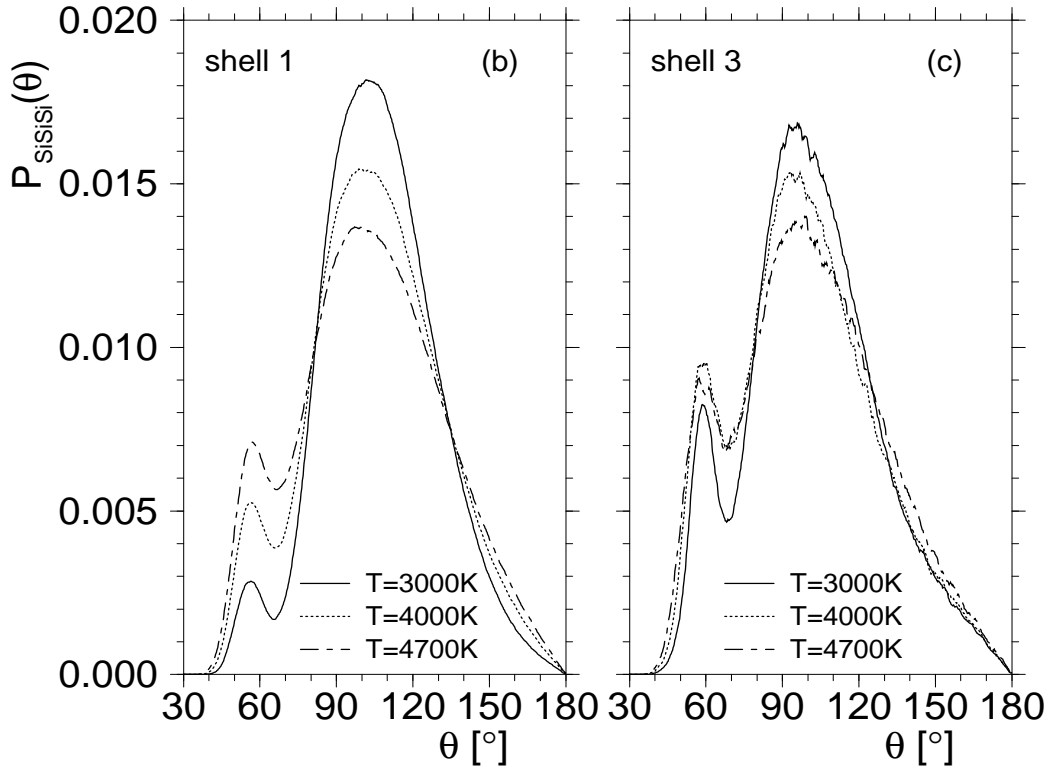
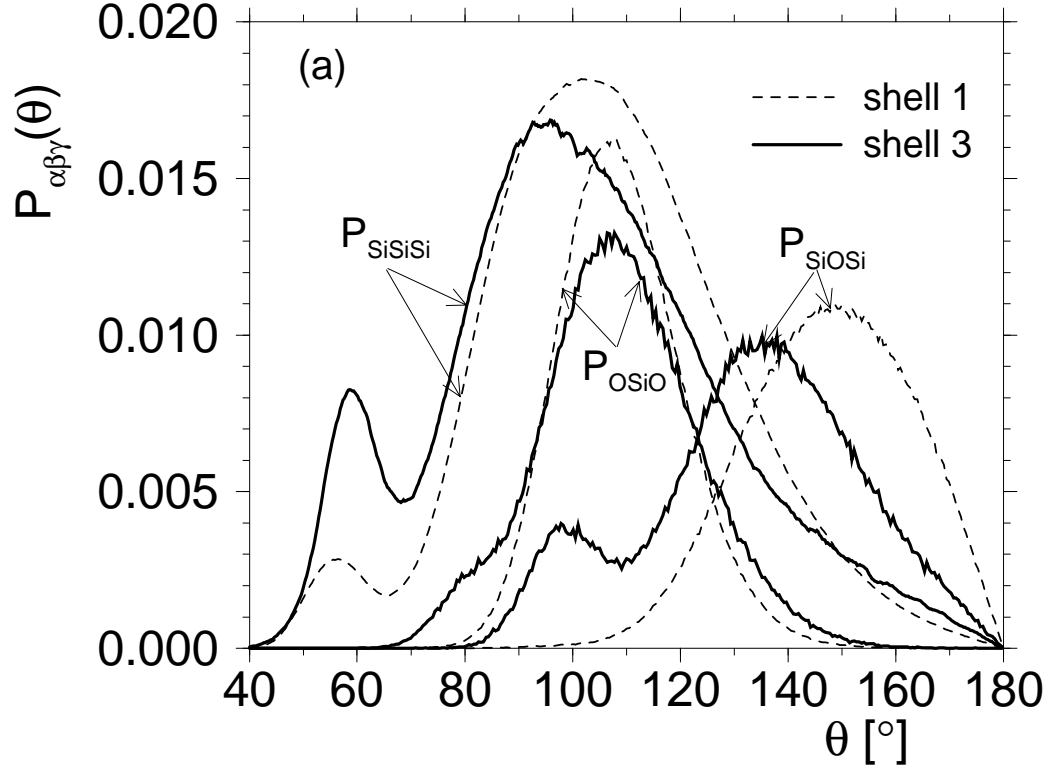


FIG. 8. Probability that an angle between neighboring atom of type α , β , and γ has a value θ for the largest system, $N = 4608$, $T = 3000\text{K}$. a) shell 1 (interior) and shell 3 (surface); b) and c) temperature dependence for shell 1 and shell 3, respectively.

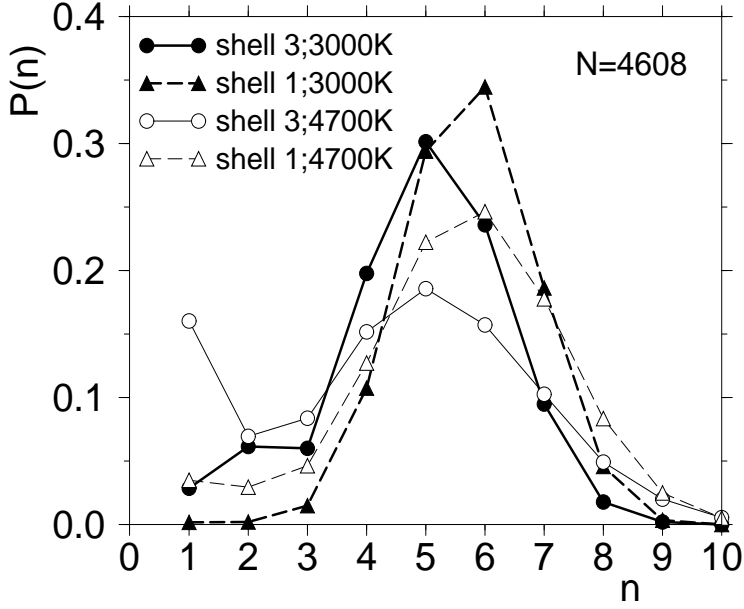


FIG. 9. Probability that a ring has length n for the case that the ring is close to the surface (circles) and is in the interior (triangles).

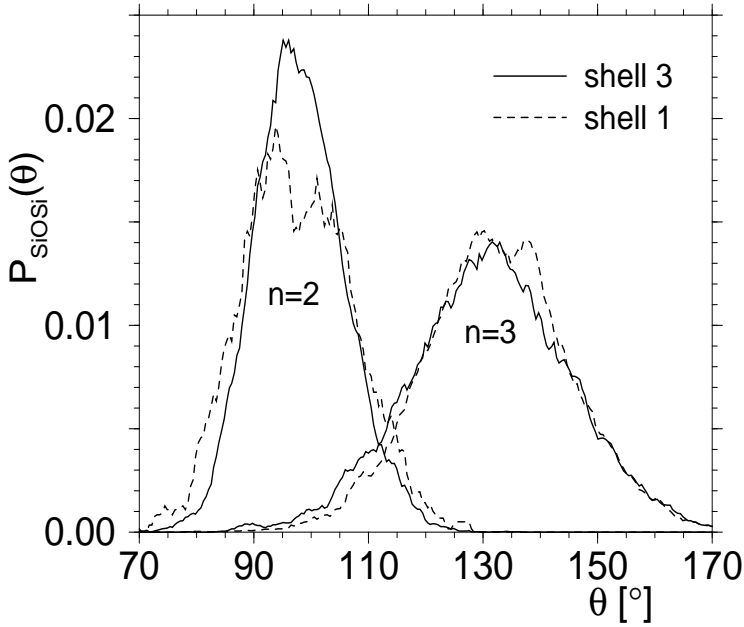


FIG. 10. Probability that in a ring of length n the angle Si-O-Si has a value θ . The solid and dashed curves are for the surface and the interior of the cluster, respectively. $T = 3000\text{K}$.

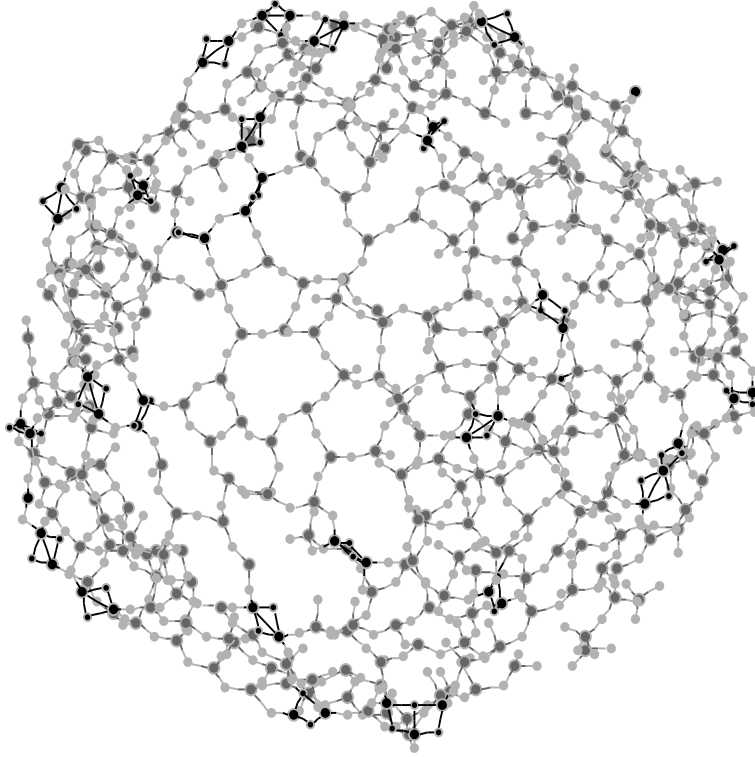


FIG. 11. Snapshot of the $N = 4608$ system at $T = 3000\text{K}$. Only the top 6\AA of the cluster are shown. Dark and light grey: silicon and oxygen atoms. Black: Two-membered rings.

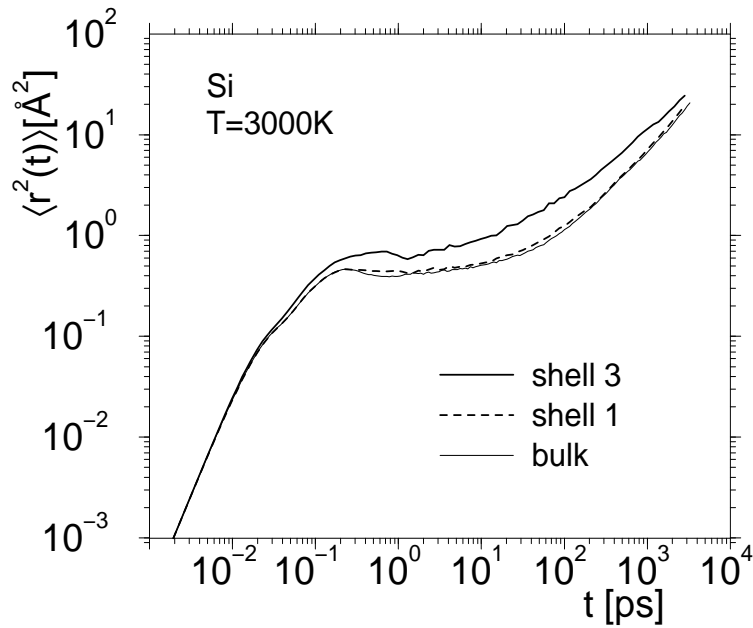


FIG. 12. Time dependence of the mean-squared displacement of a tagged silicon particle at 3000K . The bold solid and dashed curves correspond to the surface and the interior of the cluster, respectively. The thin curve correspond to the bulk [42].

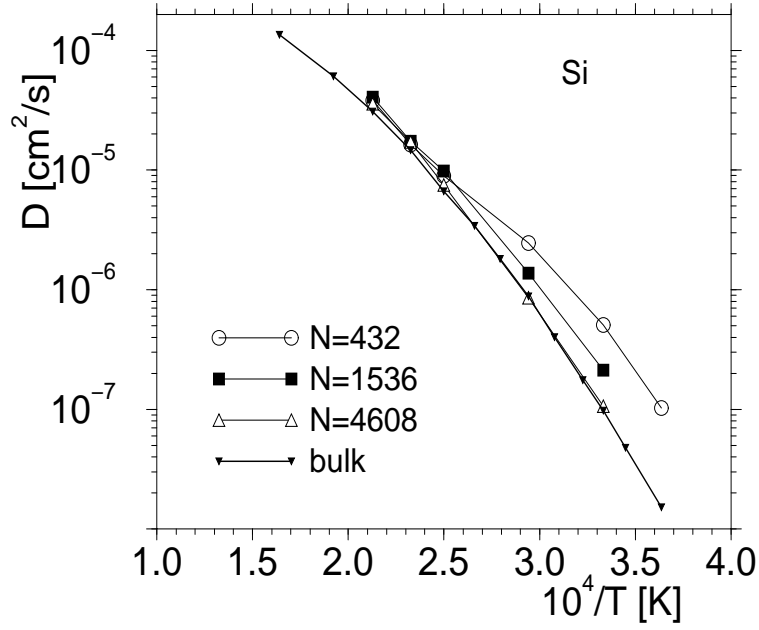


FIG. 13. Temperature dependence of the diffusion constant for the silicon atoms in the interior of the clusters. The different curves correspond to the different system sizes. Also included is the bulk data from Ref. [42].

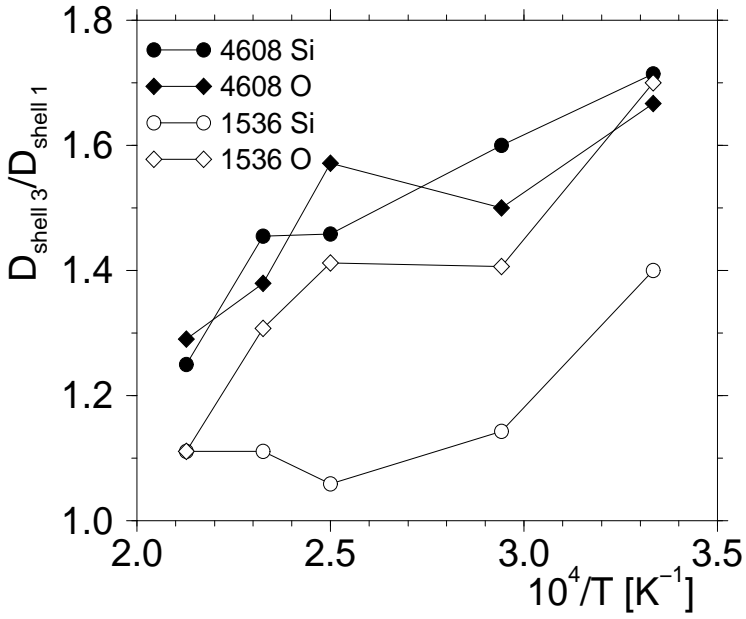


FIG. 14. Temperature dependence of the ratio between the diffusion constants in shell 3 and shell 1. The filled and open symbols are for the largest and intermediate system size, respectively.

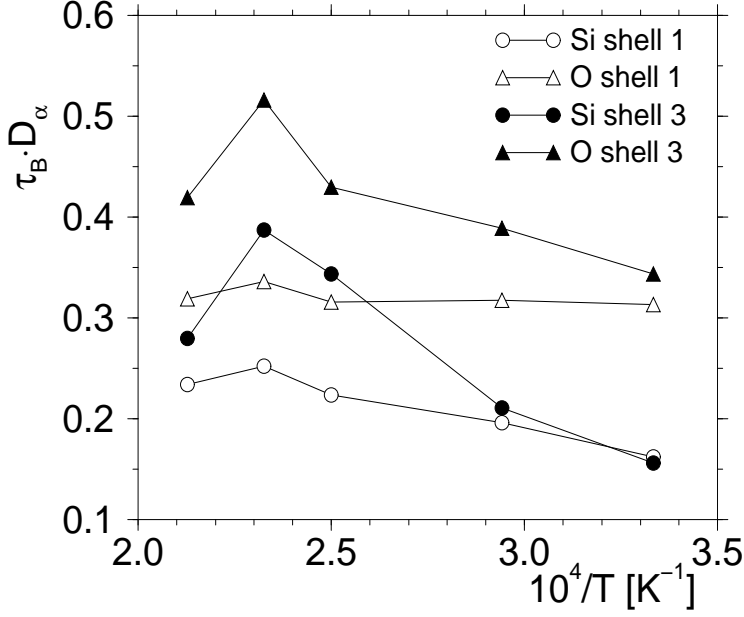


FIG. 15. Temperature dependence of the product $\tau_B(T)D_\alpha(T)$ for the interior and the surface of the cluster (open and filled symbols, respectively).

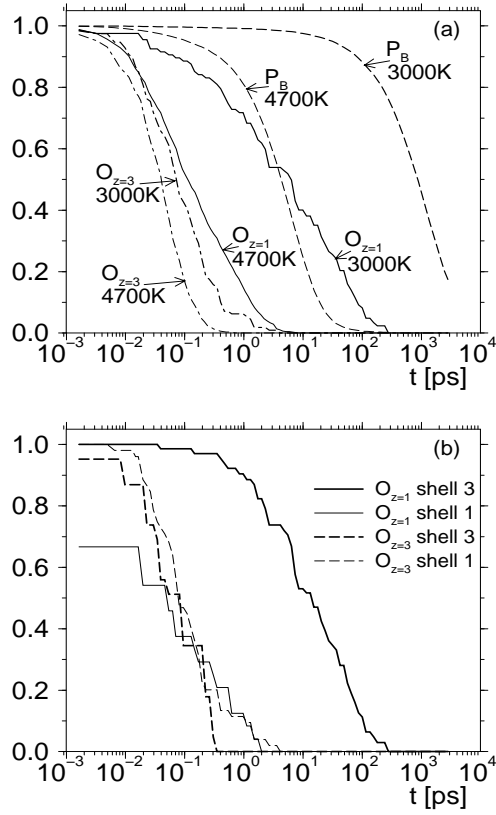


FIG. 16. Probability that a bond (curves labeled P_B) and an oxygen defect (curves labeled with $O_{z=1}$ and $O_{z=3}$) survives a time t . a) Whole system for two different temperatures. b) Dependence on the shell for $T = 3000\text{K}$.

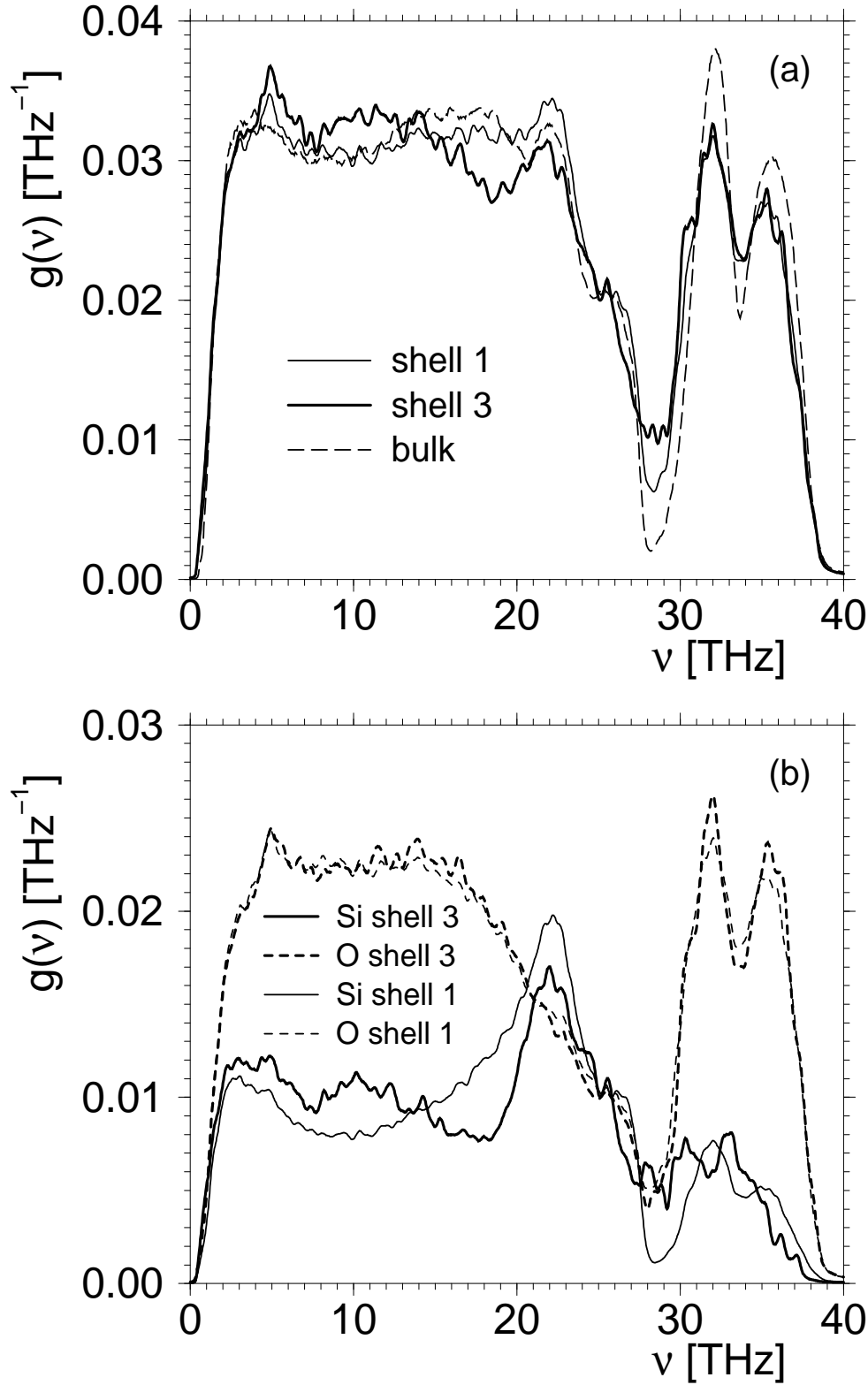


FIG. 17. Frequency dependence of the density of state. a) The atoms in shell 1 and 2. Also included are the bulk data from Ref. [41]. b) Contribution to the DOS from silicon and oxygen atoms in shell 1 and shell 3.

TABLES

	$\theta_{\text{OSiO}} [^\circ]$	$\theta_{\text{SiOSi}} [^\circ]$	$d_{\text{SiSi}} [\text{\AA}]$	$d_{\text{OO}} [\text{\AA}]$	$d_{\text{SiO}} [\text{\AA}]$
present sim.	81.5 (14)	98 (17)	2.5 (0.36)	2.28 (0.33)	1.65 (0.26)
sim. [30]	85	102		2.2	1.67
quant. [20]	88.5	91.5	2.39	2.33	1.67
quant. [21]		91.3	2.38	2.32	1.66
quant. [12]	88.5	91.5	2.39	2.33	1.67
quant. [22]	89.7	90.3			1.68
quant. [24]	89	91	2.40		1.69
exp. [56]	100.4	79.6			1.84

TABLE I. Values for the various angles and distances in a two-membered ring as determined from simulations and quantum mechanical calculations. In the first line the numbers in brackets give the width of the distribution at half maximum. The last line reports values from experiments on crystalline silica with two-membered rings.